Published in Applied Physics Letters 83, 572-574, 2003
which should be used for any reference to this work

GaN/AlN-based quantum-well infrared photodetector for 1.55 μm

Daniel Hofstetter[a] and Sven-Silvius Schad[b]
Institute of Physics, University of Neuchâtel, 1 A.-L. Breguet, CH-2000 Neuchâtel, Switzerland
Hong Wu, William J. Schaff, and Lester F. Eastman
Cornell University, Ithaca, New York 14853

We report optical absorption and photocurrent measurements on a GaN/AlN-based superlattice. The optical absorption has a full width at half maximum of 120 meV and takes place at an energy of 660 meV (5270 cm^{-1}); this corresponds to a wavelength of 1.9 μm. While the optical absorption remained unchanged up to room temperature, the photocurrent signal could be observed up to 170 K. With respect to the optical absorption, the photocurrent peak was slightly blueshifted (710 meV/5670 cm^{-1}) and had a narrower width of 115 meV. Using this quantum-well infrared photodetector, we were able to measure the spectrum of a 1.55 μm superluminescent light-emitting diode.

Optical devices based on intersubband transitions have seen a decade of tremendous progress which led, among other milestones, to the demonstration of room temperature continuously operated quantum cascade (QC) lasers,[1] far infrared QC lasers with an emission wavelength of 87 μm,[2] room temperature quantum-well infrared photodetectors (QWIPs) at 10 μm,[3] and highly sensitive infrared cameras based on arrays of QWIPs.[4] All these-impressive results have triggered the implementation of intersubband devices into "real-world" applications like optical gas sensors,[5] process monitoring systems,[6] and wireless telecommunication transmitters or receivers.[7] For the latter, there exist basically two different possibilities: one can either work in one of the atmospheric window regions and utilize, for instance, standard 10 μm QC lasers in conjunction with QWIPs or classical mercury–cadmium–telluride detectors; or use 1.55 μm interband lasers and detect the radiation with fast near-infrared (near-IR) interband or intersubband detectors. Since its conduction band discontinuity is on the order of 2 eV, the material combination AlN/GaN is the ideal material system for such near-IR itersubband detectors. Gmachl *et al.*[8] and Iizuka *et al.*[9] have demonstrated optical intersubband absorption on GaN/AlN-superlattices; they reached wavelenghts as short as 1.35 μm. Recently, our research groups in Neuchâtel and Cornell observed intersubband absorption in the triangular well of a GaN/AlGaN-based field effect transistor.[10] In yet another line of research, Gopal *et al.* showed intersubband absorption in InGaAs/AlAsSb quantum wells at wavelengths of 1.35 μm.[11] All of these devices, however, were not electrically active, which so far prevented them from being useful for practical applications. In this letter, we consequently present results on a GaN/AlN-based QWIP working at wavelengths down to 1.55 μm.

Growth of these superlattices was based on molecular beam epitaxy on c-face sapphire substrates. Thermal sources for the group III elements, and a remote radio frequency source for the atomic nitrogen were used in the epitaxy system. After a very thin AlN nucleation layer, a 500-nm-thick n-doped (Si, 5×10^{18} cm^{-3}) $Al_{0.5}Ga_{0.5}N$ buffer layer was grown, followed by a 20 period GaN/AlN superlattice with 20 Å thickness for each layer and n-doped wells (Si, nominally 5×10^{19} cm^{-3}). The top layer was a 100-nm-thick n-doped (Si, 1.5×10^{18} cm^{-3}) $Al_{0.5}Ga_{0.5}N$ layer. The compositions and the thicknesses of the superlattice were confirmed by x-ray diffraction and transmission electron microscopy (TEM). Capacitance–voltage measurements on the as-grown wafer revealed a doping level of $1-2\times10^{18}$ cm^{-3} for the top $Al_{0.5}Ga_{0.5}N$ layer; due to the relatively large thickness of the latter, the carrier density in the underlying wells could not be accurately determined. The TEM analysis revealed a certain surface roughness which did not adversely affect the optical properties of the device. After growth, the samples were metalized using a shadow mask with 800 μm wide openings. We first deposited a Ti/Al/Ti/Au (40/200/40/200 nm) ohmic contact which was annealed at 800 °C for 60 s. Between the annealed ohmic contact stripes, we evaporated stripe-shaped Pd/Au (40/200 nm) Schottky contacts. The wafer was then polished in a standard multipass waveguide geometry with two parallel 45° wedges and a polished back (see inset of Fig. 1). Due to the huge size of the contact stripes (800 μm$\times$3 mm), we observed rather large leakage currents across the diode. Using a small In dot which was squashed towards the polished edge of the wafer, we connected the ohmic top contact—and probably also the underlying superlattice and the buffer layer—to the copper submount, whereas the Schottky contact was bonded to a Au-coated ceramic contact pad. Due to the rather low lateral conductivity of the top contact layer, the superlattice was not short-circuited by the In dot.

All experiments were carried out in the sample compartment of a Nicolet Fourier-transform spectrometer (FTIR) using the internal white-light source with beam condenser, the internal room temperature deuterated triglycine sulfate detector, and the quartz beam splitter. The sample was held on the cold finger of a liquid He-flow cryostat. The background measurements for the optical absorption were done using a

[a]Electronic mail: daniel.hofstetter@unine.ch
[b]Present address: Optoelectronics Department, University of Ulm, Albert-Einstein-Allee, 89081 Ulm, Germany.

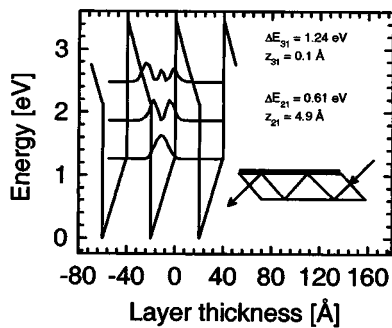

FIG. 1. Schematic conduction band structure of a GaN/AlN superlattice with 20-Å-thick well and barrier layers. The observed transition, ΔE_{21}, takes place between the ground state and the first excited state and has a computed energy of 610 meV. The inset shows a schematic cross section through the sample.

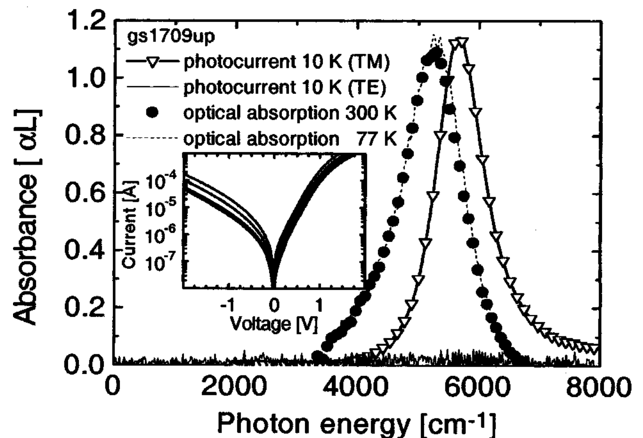

FIG. 2. Comparison between optical absorption at 300 K (circles) and at 77 K (dashed line), photocurrent at 10 K using TM polarized light (solid line with triangles), and photocurrent at 10 K using TE polarized light (solid, noisy line along the floor). The units on the y axis are valid only for the optical absorption measurements. The inset shows dark current vs bias voltage for 10 K (lowest current), 100, 200, and 300 K (highest current).

metal grid polarizer in TE orientation. For photocurrent measurements, an EG&G voltage amplifier was connected between the Schottky and the ohmic contacts of the device. Between those two electrodes, the photocurrent induced a small, but measurable voltage difference; the output of the amplifier was fed into the external detector port of the FTIR. The photocurrent experiment was done at low temperatures, typically between 10 and 170 K. For the optical absorption measurements, where no difference was seen between 77 and 300 K, we measured usually at room temperature.

In Fig. 1, we present a computed band diagram of our structure. The conduction band discontinuity was assumed to be 2.1 eV. All layer thicknesses are 20 Å, and the internal fields at each interface are ± 6.5 MV/cm.[12] The simulation was done assuming a superlattice with an infinite number of periods, no boundary effects, and no external bias voltage. Based on these assumptions, we found a transition energy of 610 meV and a dipole matrix element (an integral $[z_{21}] = \int \varphi_2^*(z) \cdot z \cdot \varphi_1(z) \cdot dz$ describing the spatial overlap between 2 electronic wave functions) of 4.9 Å between the first excited state and the ground state. Between the second excited state and the ground state, the respective numbers were 1.24 eV and 0.1 Å. Figure 2 shows a comparison between the optical absorption signal at room temperature, at 77 K, and the photocurrent measurements at 10 K for both TE, and TM-polarized light. Electromodulated absorption measurements like described in Ref. 10 were tried as well, but due to the large thickness of the top $Al_{0.5}Ga_{0.5}N$ contact layer and the high doping level in the wells, no depletion of the latter could be achieved. The optical absorption curves were obtained from measurements under both polarizations, and subsequent normalization using the formula $\alpha L = \mathrm{Log}(T_{\mathrm{TE}}/T_{\mathrm{TM}})$. T_{TE} and T_{TM} are the transmitted intensities in the two polarizations, and αL is the absorbance of the structure. From the integral under the absorbance curves, we deduced a carrier density of 6.5×10^{19} cm^{-3}; this value is consistent with the intentional doping level in the wells. In order to exclude the effects of the top metalization, optical absorption was measured in an area without metal. The absorption signal peaks at 5270 cm^{-1} (660 meV/1.9 μm) and shows a full width at half maximum (FWHM) of 120 meV. The absorption curves at 77 and at 300 K were nearly identical. Since the number of electrons in the wells remains essentially the same, the amount of optical absorption did not change. The TM photocurrent signal is slightly blueshifted with respect to the absorption, peaks at 5670 cm^{-1} (710 meV/1.76 μm) and has a FWHM of 115 meV. This blueshift is expected because optical absorption is possible as soon as the energy exceeds the transition energy, leading usually to a Lorentzian line shape. The photocurrent in our device, however, is a product between the Lorentzian absorption line shape and the tunnelling probability, which increases exponentially with decreasing barrier height. Due to this effect, the high energy tail of the initial absorption curve is enhanced quite considerably; resulting in the observed blueshift. The inset of Fig. 2 shows dark current versus bias voltage for temperatures of 10, 100, 200, and 300 K. As mentioned before, these large Schottky diodes were relatively leaky with dark current densities on the order of several tens of μA/cm^2 at low bias voltages of 0.2 V.

In order to obtain the responsivity of this QWIP, we replaced the internal white-light source of the spectrometer by a narrow emission room temperature operated 1.55 μm superluminescent light-emitting diode (SLED). In Fig. 3, we present several photocurrent measurements as a function of temperature using the white-light source; and one curve showing the emission spectrum of the SLED. The output power of the latter was set to 1 mW; this produced a photocurrent of 20 nA, resulting in a responsivity of $R = 20$ μA/W at 10 K and 1.55 μm. Assuming a coupling efficiency into the device of 1, we deduce a peak responsivity of $R_i = 100$ μA/W.[13] Based on a 10 K device resistance of 8.1 MΩ, and considering Johnson noise as the dominant noise source ($\mathrm{NEP} = I_{n,\mathrm{Johnson}}/R_i = 45$ nW), this results in a detectivity of roughly 2×10^9 (cm^2 Hz)$^{1/2}$/W. Knowing further the quantum efficiency of $\eta = 0.68$, the conversion factor $e/h\nu = 1.41$ A/W, the capture probability of $p_c = 1$, and the number of QWs, $N = 20$, we were able to estimate the escape probability $p_e = (N p_c R_i)/(e\eta/h\nu) = 0.002$. Given the barrier height of more than 1 eV in our structure, this small value looks quite reasonable.

Figure 4, finally, shows the photocurrent versus photon energy curves as a function of temperature up to 170 K. In the inset, we present peak signal height versus bias voltage

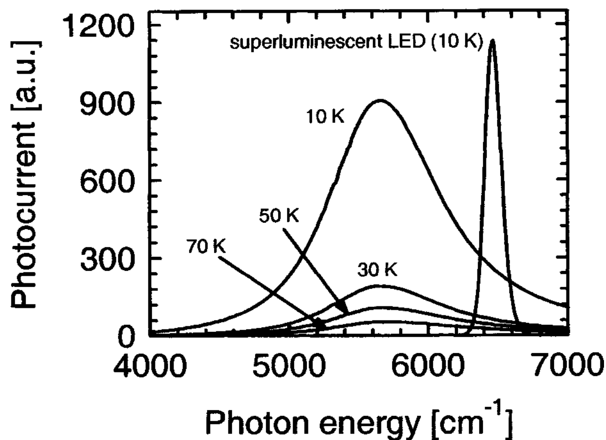

FIG. 3. Photocurrent vs photon energy curves for temperatures of 10, 30, 50, and 70 K. The peaked signal at 1.55 μm was obtained using an external SLED ($P=1$ mW, $T=300$ K) as excitation source.

(left half) and versus temperature (right half). Under application of a positive bias voltage, the photocurrent increased slightly, namely by about 25% for a voltage of $+0.7$ V on the Schottky contact. Likewise, a signal decrease of about 30% could be observed under application of a negative voltage of -0.6 V. Based on these observations, we concluded that the direction of the unbiased photocurrent is from the top contact towards the buffer layer. For higher voltages of both polarities, the signal became increasingly noisy, and no additional measurements were possible. Especially at very low temperatures, a small shoulder on the high energy tail of the main peak became visible. The approximate energy of 9500 cm^{-1} and its small relative height, only about 5% of the main peak, are consistent with what we predicted for the slightly diagonal ΔE_{31} transition in the quantum wells. Due to the greatly reduced residual barrier height/thickness and thus the much higher tunnelling probability, even this transition with its extremely small oscillator strength could contribute to the photocurrent.

When going up to 170 K, the sensitivity dropped by about two orders of magnitude. A likely reason for this observation is the internal device resistance which eventually gets too low, so that the signal becomes of comparable size as the Johnson noise. A classical QWIP has its excited state resonantly aligned with the upper band edge. This guarantees a high escape probability of the electrons, lowers their capture probability, and allows to improve the responsivity by applying a voltage on the structure. In our case, the upper state is still more than 1 eV below the upper band edge. Thus, a very low probability tunnelling process is necessary to enable current flowing across the superlattice. As seen above, we estimated $p_e=0.002$ for this probability. From this point of view, a GaN/AlN QWIP at 1.76 μm suffers from a similar performance problem as a QC laser used as photodetector.[13] The photoconductive gain is also low because the electrons will have a high capture, but a very low escape probability. The naive estimation mentioned before resulted indeed in $g_{\text{photo}}=10^{-4}$. We therefore expected a low responsivity, and only a marginal improvement under application of a small bias voltage; in agreement with the experimental findings. However, since the noise gain is small as well, the noise behavior is quite good, which is confirmed by the detectivity value of 2×10^9 (cm^2 Hz)$^{1/2}$/W.

In conclusion, we have presented a GaN/AlN-based QWIP which is most sensitive at a wavelength of 1.76 μm. Using this structure, we were able to measure the emission spectrum of a 1.55 μm SLED. This result is an extremely important milestone towards the demonstration of a high performance intersubband detector at the telecommunication wavelength of 1.55 μm.

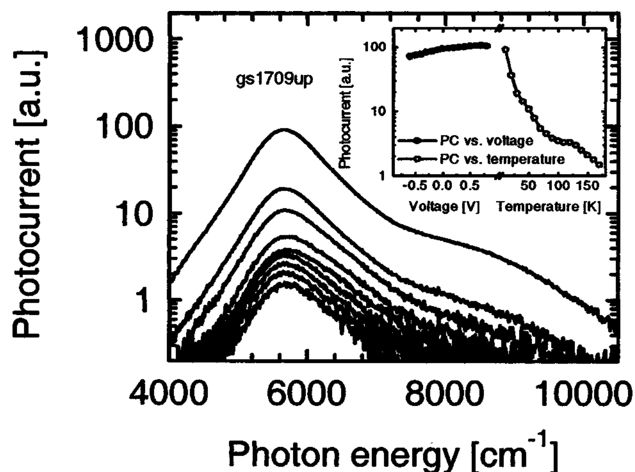

FIG. 4. Photocurrent vs photon energy curves, at zero bias voltage and different temperatures in steps of 20 K from 10 K (highest signal) to 170 K (lowest signal). The inset shows the peak photocurrent signal as a function of different bias voltages (left) at 10 K; and as a function of temperature at zero bias (right).

The authors gratefully acknowledge valuable discussions with Lubos Hvozdara (Alpes Lasers, SA, Neuchâtel), Xavier Niquille, and Jérôme Faist (both Uni NE), and funding from the Professorship Program of the Swiss National Science Foundation, the ONR NICOP program, Contract No. N00014021095 of the US Office of Naval Research, and NSF Project No. 0123453.

[1] M. Beck, D. Hofstetter, T. Aellen, J. Faist, U. Oesterle, M. Ilegems, E. Gini, and H. Melchior, Science **295**, 301 (2002).
[2] L. Ajili, G. Scalari, D. Hofstetter, M. Beck, J. Faist, H. Beere, G. Davis, E. Linfield, and D. Ritchie, Electron. Lett. **38**, 1675 (2002).
[3] H. C. Liu, R. Dudek, A. Shen, E. Dupont, C. Y. Song, Z. R. Wasilewski, and M. Buchanan, Appl. Phys. Lett. **79**, 4237 (2001).
[4] S. D. Gunapala, S. V. Bandara, J. K. Liu, W. Hong, M. Sundaram, P. D. Maker, R. E. Muller, C. A. Shott, and R. Carralejo, IEEE Trans. Electron Devices **45**, 1890 (1998).
[5] D. D. Nelson, J. H. Shorter, J. B. McManus, and M. S. Zahniser, Appl. Phys. B: Lasers Opt. **B75**, 343 (2002).
[6] A. A. Kosterev and F. K. Tittel, IEEE J. Quantum Electron. **38**, 582 (2002).
[7] R. Martini, R. Paiella, C. Gmachl, F. Capasso, E. A. Whittaker, H. C. Liu, H. Y. Hwang, D. L. Sivco, J. N. Baillargeon, and A. Y. Cho, Electron. Lett. **37**, 1290 (2001).
[8] C. Gmachl, H. M. Ng, and A. Y. Cho, Appl. Phys. Lett. **79**, 1590 (2001).
[9] N. Iizuka, K. Kaneko, N. Suzuki, T. Asano, S. Noda, and O. Wada, Appl. Phys. Lett. **77**, 648 (2000).
[10] D. Hofstetter, L. Diehl, J. Faist, J. Hwang, W. J. Schaff, L. F. Eastman, and C. Zellweger, Appl. Phys. Lett. **80**, 2991 (2002).
[11] A. V. Gopal, H. Yoshida, T. Simoyama, N. Georgiev, T. Mozume, and H. Ishikawa, Appl. Phys. Lett. **80**, 4696 (2002).
[12] O. Ambacher, B. Foutz, J. Smart, J. R. Shealy, N. G. Weimann, K. Chu, M. Murphy, A. J. Sierakowski, W. J. Schaff, L. F. Eastman, R. Dimitrov, A. Mitchell, and M. Stutzmann, J. Appl. Phys. **87**, 334 (2000).
[13] D. Hofstetter, M. Beck, and J. Faist, Appl. Phys. Lett. **81**, 2683 (2002).